



The Failure of Sn-Bi-Based Solder Joints Due to Current Stressing

Faramarz Hadian¹ · Sitaram Panta¹ · Javier Flores¹ · Eric J. Cotts¹

Received: 18 May 2022 / Accepted: 10 November 2022 / Published online: 3 December 2022
© The Minerals, Metals & Materials Society 2022

Abstract

The electrical resistances of Cu/Sn57BiSbNi/Ni solder joints were continuously monitored during current stressing at temperatures between 95 and 125°C, and current densities up to 7kA/cm², for times approaching 3000 h. Scanning electron microscopy was utilized to characterize corresponding changes in solder joint microstructure. The statistics of failure based upon a 20% increase in electrical resistance (correlated with the growth of a continuous layer of Bi at the anode) were analyzed for groups of nominally identical samples, while either current density or temperature was independently varied. At longer times, after prodigious, diffusion-limited growth of a Cu₆Sn₅-based phase, catastrophic failure (an increase in electrical resistance of 20 mΩ) was observed and correlated with crack propagation across the width of the sample. The statistics of catastrophic failure were analyzed during current stressing of these SnBi-based solder joints at a relatively high temperature (125°C) and current density (4kA/cm²).

Keywords Low-temperature solders · current stressing · failure analysis · atomic diffusion · electrical resistivity · phase transformations

Introduction

Sn-Bi-based Pb-free solders offer promise for low-temperature assembly.^{1,2} For instance, the eutectic Sn-58Bi solder alloy enables process temperatures as low as 140°C (175–190°C is more common), and is widely available in paste form (e.g., Sn-57Bi-1Ag).^{3–5} The mechanical properties of Sn-XBi alloys depend upon the Bi weight percent, X. For instance, the addition of small amounts of Bi to Sn dramatically increases shear strength, the shear strength of Sn-2.5Bi being almost twice that of Sn.^{6,7} Furthermore, the elongation of Sn-X Bi alloys was observed to vary significantly with X,⁸ and Coyle et al. reported significant effects of X on the lifetime in accelerated thermal cycling of SAC/SnBi mixed solder joints.^{2,9} Given the sensitivity of the mechanical properties of SnBi-based solder joints to the distribution of Bi in the Sn, more examination is needed of Bi migration during current stressing. In the field, SnBi solder joints are subjected to current densities up to and exceeding 2000 A/cm², and operating temperatures up to

100°C.^{3,4} Such current stressing causes Bi precipitates in the bulk to coarsen, as well as the accumulation of Bi at the anode, resulting in changes in the mechanical properties of the solder joint.^{2,10–16}

Segregation of Bi at the anode was also correlated with a large increase in the electrical resistance of the solder joint.^{17–21} In fact, failure criteria during current stressing focus on specific increases in the electrical resistance of the SnBi-based solder joint. For example, a 20% increase in the electrical resistance of a SnBi solder joint is a common choice of a failure criterion during current stressing.^{22–25} The kinetics of failure for such a failure criterion have been previously quantified:^{26,27}

$$\text{MTF} = \frac{1.9 \times 10^{-7}}{j} \exp\left(\frac{0.98 \text{ eV/atom}}{kT}\right) \text{h} \quad (1)$$

This previous study²⁷ found that the mean time to failure (MTF) during current stressing varied systematically with current density, *j*, and temperature, *T* (Eq. 1, where MTF is expressed in hours, *j* in amperes per square centimeter, and temperature in Kelvin). The apparent activation energy was 0.98 eV/atom, where *k* is Boltzmann's constant in eV/K. However, little examination of the statistics of these failures has been provided. Furthermore, a study of the nature of catastrophic failure is needed, where the failure criterion

✉ Eric J. Cotts
ecotts@binghamton.edu

¹ Department of Physics and Materials Science, Binghamton University, Binghamton, NY, USA

generally rests on a fixed, substantial increase in electrical resistivity, e.g., 20 m Ω . Therefore the present work has focused on the statistics and kinetics of failure of SnBi-based solder joints during current stressing, and correlated microstructural changes.

Experimental

Near-eutectic Sn57Bi + 0.5Sb0.01Ni solder paste was used to assemble cylindrical solder joints, using conventional surface mount technology. The samples were individual, 230- μ m-diameter, solder mask-defined solder joints, each with a custom-made laminate chip on a laminate board. The metallization on the component side was electroless nickel immersion gold (ENIG), with a Cu metallization on the board. This custom-made laminate chip sample geometry (Fig. 1) allowed four-terminal measurements of the electrical resistance of individual solder joints to be conducted. The reflow process was performed in an IR 10 zone reflow machine (RF-430-N2; Japan Pulse Laboratory). Assemblies were reflowed with a peak temperature, T_p , equal to 190°C. The time above liquidus was approximately 60 s.

The electromigration test was performed using a DC power supply (Agilent E3649E), with the constant electrical current applied to the rows of the solder joints in series. Each row had 10 solder joints, including feeding joints, jumpers, and risk sites (Fig. 1). Four terminal measurements were performed to monitor the electrical resistance versus time of individual joints while they were stressed with a constant current, at a constant temperature. Typically, 30 risk sites were monitored for any particular

set of parameter values. The temperatures of the solder joints during current stressing were determined by placing a thermocouple (OM-CP-OCTPRO; Omega) close to the solder joint under stress, and by using the TCR method (JESD33B).²⁸ Metallographic cross-sectional analysis with scanning electron microscopy (SEM) was used to characterize the evolution of the solder microstructures at the given current stressing time.

Results and Discussion

Microstructure of as-Reflowed Sn57BiSbNi Solder Joints

The microstructure of Sn57BiSbNi solder joints was characterized after reflow by means of SEM (Fig. 2). The height of each solder joint was approximately 76 μ m and the radius 115 μ m (Fig. 2). The SEM micrographs revealed a phase mixture consisting of interspersed, nearly equal volumes of irregularly shaped Bi (white) and Sn(Bi) (gray) precipitates. Closer examination (Fig. 2) revealed that the length scale of the near-eutectic SnBi phase was approximately 5 μ m. Intermetallic compounds were visible at the SnBi/metallization interfaces (Fig. 2). The composition of the IMC at the ENIG/SnBi interface was found to be (CuAuNi)₆Sn₅. A Cu₆Sn₅ phase was also observed at the Cu/SnBi interface, although much less Ni was found in this phase. The atomic percentages were approximately 47%Sn with 30% Cu, 20%Ni, and 3%Au, corresponding fairly well to (Cu,Ni,Au)₆Sn₅.

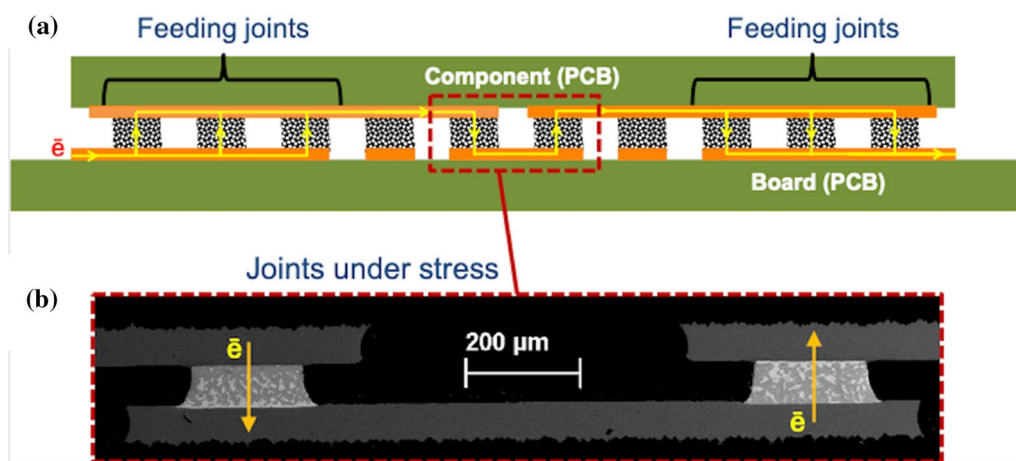


Fig. 1 (a) Schematic of a row of solder joints under current stressing in the test vehicle, including feeding joints, jumpers, and risk sites; yellow arrow the direction of electron flow during electromigration. (b) Scanning electron micrograph of an actual cross-sectioned risk

sites area corresponding to (a). The current was from component to board in one joint, and from board to component in the other joint (Color figure online).

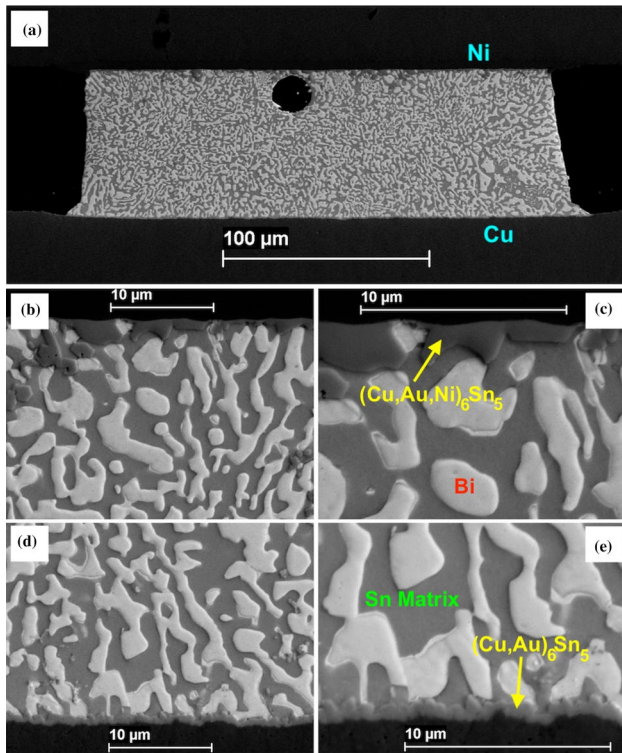


Fig. 2 SEM micrographs of an as-reflowed Cu/Sn57BiSbNi/Ni solder joint. The micrographs reveal the Bi phase (white) interspersed with the Sn(Bi) phase (gray): (a) cross-section of the solder joint after reflow; (b–e) higher-magnification micrographs providing some detail of the intermetallic compounds formed at the metallization/solder interfaces: (b) Sn57BiSbNi/Ni interface, (c) Sn57BiSbNi/Ni interface, (d) Cu/Sn57BiSbNi interface, and (e) Sn57BiSbNi/Ni interface (Color figure online).

Microstructure of as-Reflowed Sn57BiSbNi Solder Joints

Four terminal measurements of the electrical resistance of the as-reflowed Cu/Sn57BiSbNi/Ni solder joints were performed at temperatures from 95°C to 125°C (Fig. 3). At a temperature of 125°C, the values of the electrical resistances of the solder joints varied from 2.3 to 2.6 mΩ. These measured electrical resistances primarily reflected the electrical resistance of the SnBiSbNi solder, but also included the electrical resistances of the IMC layers at the metallization/solder boundaries, and a small section of the Cu traces. The average value of the electrical resistance after reflow increased monotonically with temperature (Fig. 3b); the observed increase was consistent with the temperature coefficient of the electrical resistance for Sn, Bi, and Cu (0.4%/°C).

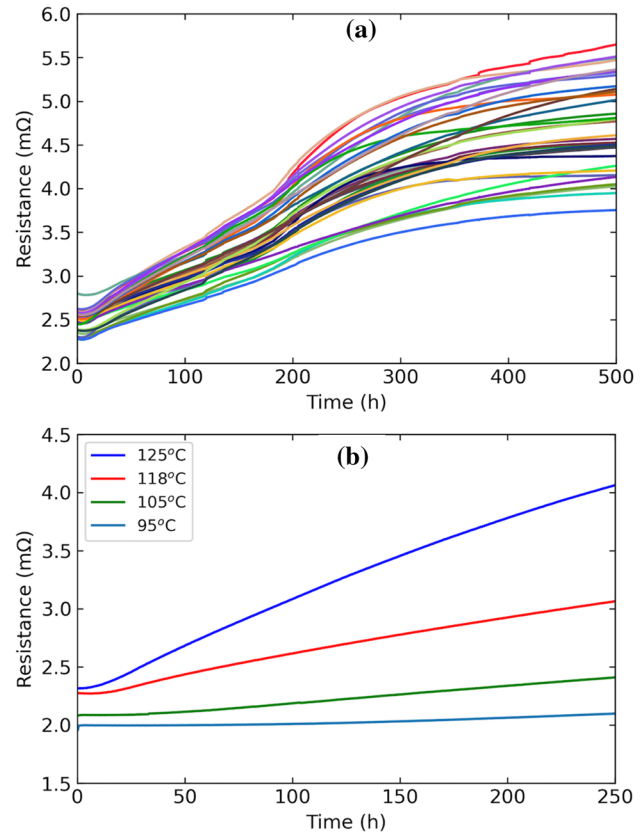


Fig. 3 (a) Electrical resistance versus time of a number of Cu/Sn57BiSbNi/Ni solder joints during current stressing at a temperature of 125°C and a current density of 4kA/cm²; (b) average electrical resistance versus time for a number of Cu/Sn57BiSbNi/Ni solder joints during current stressing at different temperatures, and a current density of 6kA/cm².

Change in Electrical Resistance with Time of Sn57BiSbNi Solder Joints During Current Stressing

The general behavior of the electrical resistance of a Cu/Sn57BiSbNi/Ni low-temperature solder joint during the early stages of current stressing is illustrated by the four terminal measurements of individual solder joints in the first 500 h of current stressing (Fig. 3a). Although there were distinct variations between individual resistance versus time curves (Fig. 3a), the electrical resistance of each solder joint increased monotonically with time. For the first 250 h, the average slope of the curves was 6 μΩ/h at a temperature of 125°C (Fig. 3a and b). It is evident that, given a failure criterion of a 20% increase in electrical resistance, all the solder joints reflected in Fig. 3a failed during the exhibited runs, with an average failure time of approximately 100 h. At later times (Fig. 3a), the electrical resistance continued to increase with time, although generally at a lower rate.

The effects of temperature on the electrical resistance versus time curves during current stressing for these Sn57BiSbNi solder joints are reflected in Fig. 3b, with averages of curves for 6 kA/cm^2 for four different temperatures. The temperature dependence of the initial electrical resistance, R_0 , is evident, as is the temperature dependence of the rate of change of the electrical resistance as a function of time. Individual resistance versus time curves in Fig. 3b are similarly shaped. Initially, a plateau was observed (e.g., for over 50 h at 95°C and for approximately 5 h at 125°C). Then, the rate of change of resistance versus time increased with time until reaching a constant rate, i.e., after the initial transients, a constant rate of change of electrical resistance versus time was observed. This rate increased with temperature (Fig. 3b). It was found that an extrapolation back to zero time of a line to this region of resistance versus time data intercepted the y axis at essentially a resistance of R_0 . The slope of the curves after the initial transients increased with temperature, the rate for 125°C was more than 10 times that observed at a temperature of 95°C .

Plots of the electrical resistance versus time, for times up to 2600 h, are presented in Fig. 4. A fairly steady rate of increase in the electrical resistance of a particular solder joint was generally observed at later times (after 500 h), until such time that the electrical resistance underwent a sharp increase, as evident in Fig. 4. In fact, Fig. 4 reveals electrical resistance versus time curves for three different SnBi-based solder joints that exhibited such behavior, with the precipitous increase in electrical resistance at distinctly different times. The maximum value of electrical resistance presented in Fig. 4 exceeded a standard failure, criterion-based upon achieving a single solder joint electrical resistance of $20 \text{ m}\Omega$. Such a relatively large increase in electrical resistance may be termed a catastrophic failure.

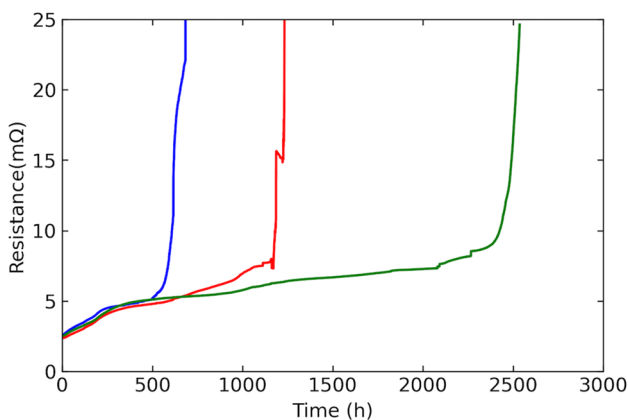


Fig. 4 Electrical resistance versus time of three Cu/Sn57BiSbNi/Ni solder joints during current stressing at a temperature of 125°C and a current density of 4 kA/cm^2 .

Change in Microstructure with Time of Sn57BiSbNi Solder Joints During Current Stressing

Significant changes in the microstructure of Cu/Sn57BiSbNi/Ni solder joints were observed with current stressing. At early times ($t < 500 \text{ h}$), Bi accumulated at the anode of the solder joint, while intermetallic compounds (IMCs) grew at the metallization interfaces (Figs. 5 and 6). For instance, Bi accumulated steadily for up to 400 h at the anode of Sn57BiSbNi solder joints at a temperature 125°C and a current density of 4 kA/cm^2 (Figs. 4a–c and 5a–c, yellow arrows indicate the direction of electron flow). This behavior was similar for electron currents from the Cu metallization to the Ni metallization (termed ‘up’) and for electron currents in the opposite direction (‘down’). For example, Bi layers tens of microns thick were observed after only 400 h of current stressing at a current density of 4 kA/cm^2 at a temperature of 125°C in the Cu/Sn57BiSbNi/Ni samples (Fig. 5). Similar results for the Bi accumulation were observed for electron current ‘down’ (Fig. 6). The majority of the Bi atoms in the SnBi-based solder had been transferred to the anode side after 400 h of current stressing, although a significant amount of Bi (approximately 20 wt%) remained in the Sn at this time.

IMCs grew at metallization interfaces during current stressing (Figs. 5 and 6). Initially, Cu_6Sn_5 formed at the Cu metallization and $(\text{Cu,Ni})_6\text{Sn}_5$ formed at the Ni metallization (an approximately $1\text{-}\mu\text{m}$ -thick layer of each phase formed during reflow; Fig. 2). Subsequent growth behavior of IMCs was strongly dependent upon the direction of the electron current. When the electron current was up (Fig. 5), limited growth of the $(\text{Cu,Ni})_6\text{Sn}_5$ layer at the anode was observed during current stressing. That is to say, only a $1\text{-}\mu\text{m}$ -thick layer of $(\text{Cu,Ni})_6\text{Sn}_5$ was observed between the Bi layer and the ENIG metallization after long periods of current stressing at 4 kA/cm^2 at 125°C . When the electron current was down (Fig. 6), the IMC at the Ni metallization was observed to thicken somewhat during current stressing, tripling in thickness after 2000 h, while the thickness of the IMC at the Cu metallization was limited.

At later times ($t > 500 \text{ h}$), in samples with the electron current flowing away from the Cu metallization (up; Fig. 5d–f), the rate of Bi accumulation was observed to be an order of magnitude slower than that initially observed during current stressing (e.g., Fig. 5a–c), while the formation of the Cu_6Sn_5 phase at Cu/Sn57BiSb interfaces in current up samples continued to the point of consuming all the Sn in the solder joint. For instance, after current stressing at 4 kA/cm^2 for 800 h, an approximately $30\text{-}\mu\text{m}$ -thick layer of Cu_6Sn_5 had formed at the cathode (Fig. 5d). Continued current stressing, for times up to 2500 h (Fig. 5f), resulted in the formation of a layer of Cu_6Sn_5 approximately $50 \mu\text{m}$ thick near the Cu metallization. Essentially, all the Sn had

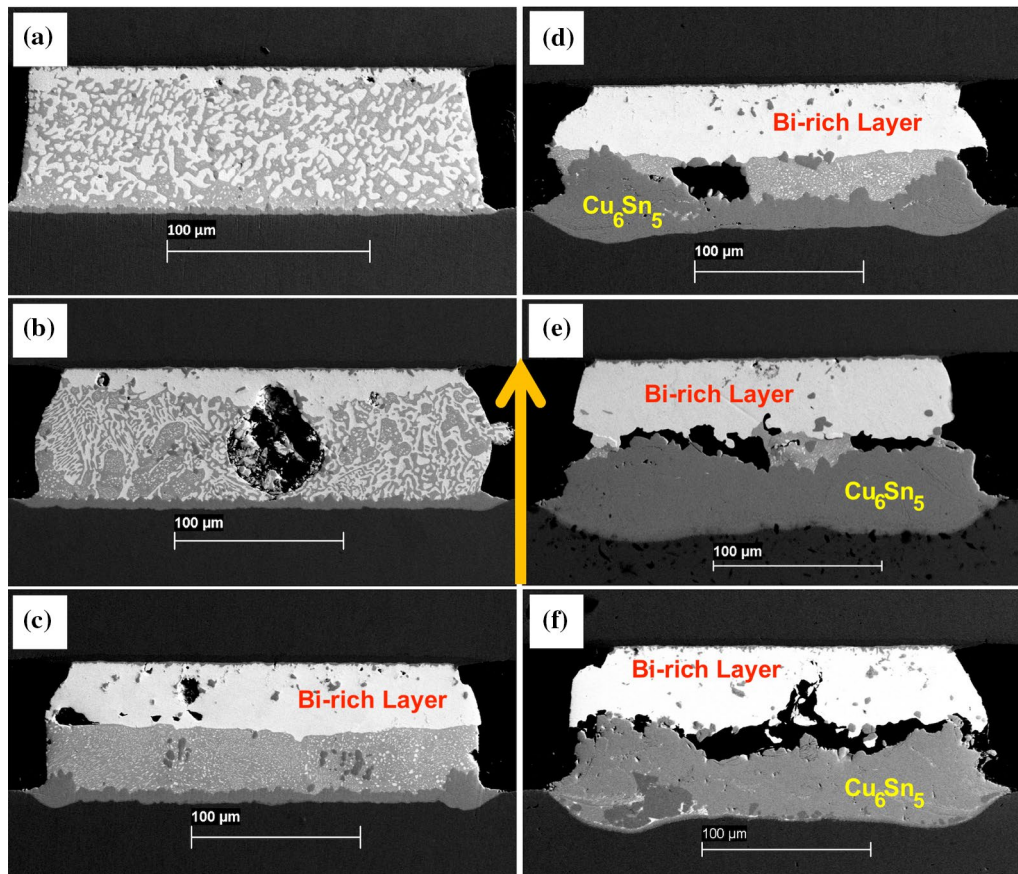


Fig. 5 Scanning electron micrographs of Cu/Sn57BiSbNi/Ni solder joints which had been current-stressed for (a) 100 h, (b) 200 h, (c) 400 h, (d) 800 h, (e) 2200 h, and (f) 2500 h at a temperature of 125°C

and a current density of 4kA/cm²; yellow arrow the electron current direction (up) (Color figure online).

been converted into Cu-Sn IMCs (a limited amount of Cu₃Sn formed between the Cu₆Sn₅ phase and the Cu metallization, as would be expected). In sharp contrast to this behavior, when the electron current was towards the Cu metallization (down; Fig. 6d–f), only a limited thickness of Cu₆Sn₅ phase formed at the Cu metallization.

In those solder joints with the electron current towards the Ni metallization (current up), catastrophic failure was observed after consumption of essentially all the Sn in the formation of Cu₆Sn₅. Such an event was associated with a volumetric reduction and an associated mechanical stress.^{29,30} In fact, a separation (crack) was observed along the interface of the Bi and Cu₆Sn₅ phase in the current up samples (Fig. 5). In the current down samples, a significant thickness of the Sn(Bi) phase sometimes remained for long periods (e.g., Fig. 6e, 2200 h). In other current down samples, essentially all the Sn had been converted to an IMC, and separation was observed at the Bi/IMC interface (e.g., Fig. 6f, 2500 h). A large (catastrophic, i.e., greater than 20-mΩ increase in electrical resistance) was observed concurrently with cracking at the Bi interface (Fig. 4 shows

plots of resistance versus time with relatively rapid increases in electrical resistance corresponding to such an event).

Failure Analysis of Cu/Sn57BiSbNi/Ni Solder Joints During Current Stressing

Failure analysis was performed after measurements of the electrical resistance of nominally identical Cu/Sn57BiSbNi/Ni solder joints during current stressing, using one of two different failure criteria. The first criterion to be utilized was a 20% increase in electrical resistance (as measured using a four-terminal technique). After a relatively short time during current stressing of SnBi-based solder joints (e.g., 10 h at a temperature of 125°C and a current density of 4kA/cm², Figs. 3a, and 5), Bi began to accumulate at a linear rate at the anode. The corresponding increase of electrical resistance of the solder joint may be deleterious to the electrical performance of the package. Other concerns are about the existence of a continuous layer of relatively pure Bi near the metallization interface, as interfaces between Bi and IMCs may be susceptible to cracking when subjected to drop

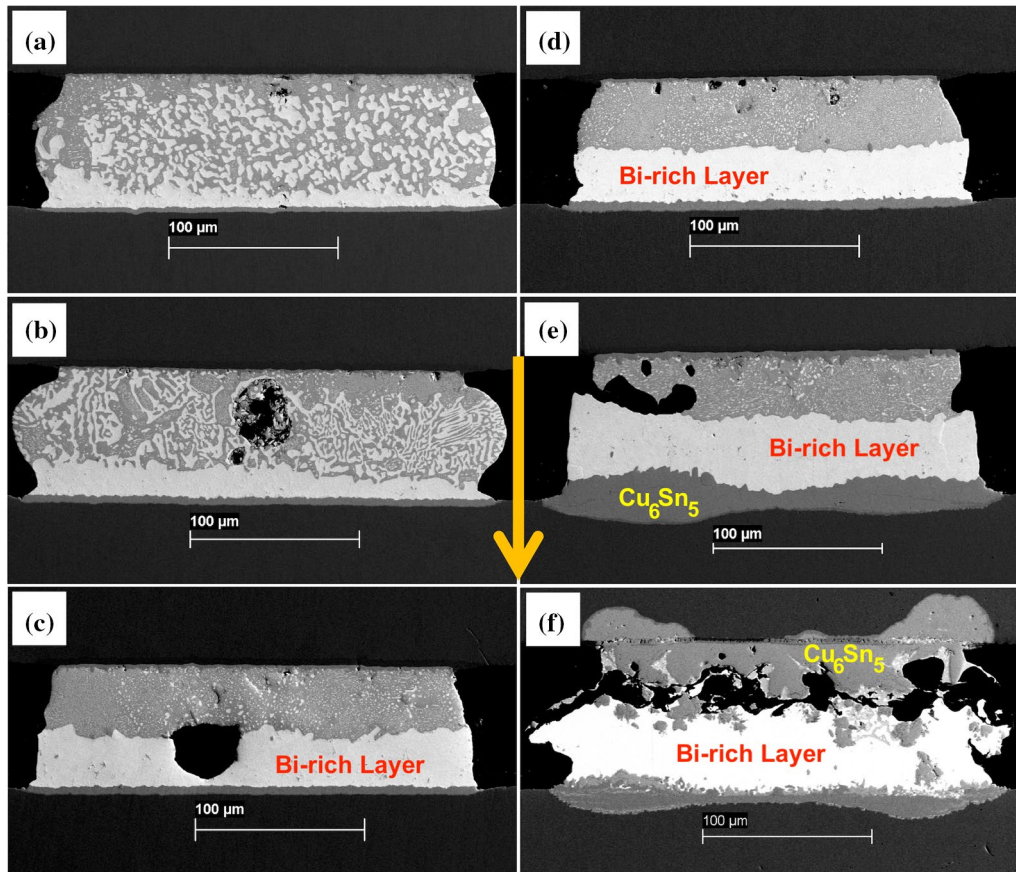


Fig. 6 Scanning electron micrographs of Cu/Sn57BiSbNi/Ni solder joints which had been current-stressed for (a) 100 h, (b) 200 h, (c) 400 h, (d) 800 h, (e) 2200 h, and (f) 2500 h at a temperature of 125°C

and a current density of 4kA/cm² yellow arrow the electron current direction (down) (Color figure online).

shock. The deleterious nature of the second type of failure during current stressing was clear, as it corresponded to the formation of very large cracks, and a precipitous (20-mΩ) increase in electrical resistance of these SnBi-based solder joints. Such failures were observed in the Cu/Sn57BiSbNi/Ni solder joints at much longer times (Fig. 4).

Times to failure were found for a 20% increase in electrical resistance of Cu/Sn57BiSbNi/Ni solder joints using four-terminal measurements of electrical resistance and careful temperature measurements. Current densities varied from 4 to 7 kA/cm² and temperatures from 95 to 125°C. The results of this fitting process using the Weibull analysis are presented in Figs. 7 and 8. The variation in failure distributions upon change in the temperature of similar samples is presented in Fig. 7. All the samples in Fig. 7 were current-stressed at 6kA/cm², while the data were analyzed in four separate groups, corresponding to each sample's temperature (sample temperatures ranged from 95 to 125°C). The standard deviations of the time to failure ranged from 20 to 40% of the MTF (Fig. 7). The effect of a 2% increase in temperature (on the Kelvin scale) was clearly discernible

on the MTF (it decreased by a factor of two), as expected in a process dominated by the thermally activated process of atomic diffusion.²⁷

Systematically varying the current density (while holding the temperature constant) during current stressing, also resulted in a systematic variation of the MTF. An increase of the current density by 1 kA/cm² resulted in a distribution of failure times, which was clearly biased to shorter times (Fig. 8). In fact, as expected from a simple Black's equation picture, the MTF was inversely proportional to the current density (Fig. 8), i.e., the MTF for samples current-stressed at a current density of 7kA/cm² was almost half that of samples tested at 4kA/cm² (Fig. 8).

Catastrophic failure (a 20-mΩ increase in electrical resistance) of a set of the Cu/Sn57BiSbNi/Ni samples took an order of magnitude longer than a 20% increase in the electrical resistance of the sample. At a temperature of 125°C, data were gathered on both processes in a reasonable length of time (Fig. 9). A total of 37 solder joints were tested using the catastrophic failure criterion; when more than 50% of the joints for a particular board passed the failure threshold

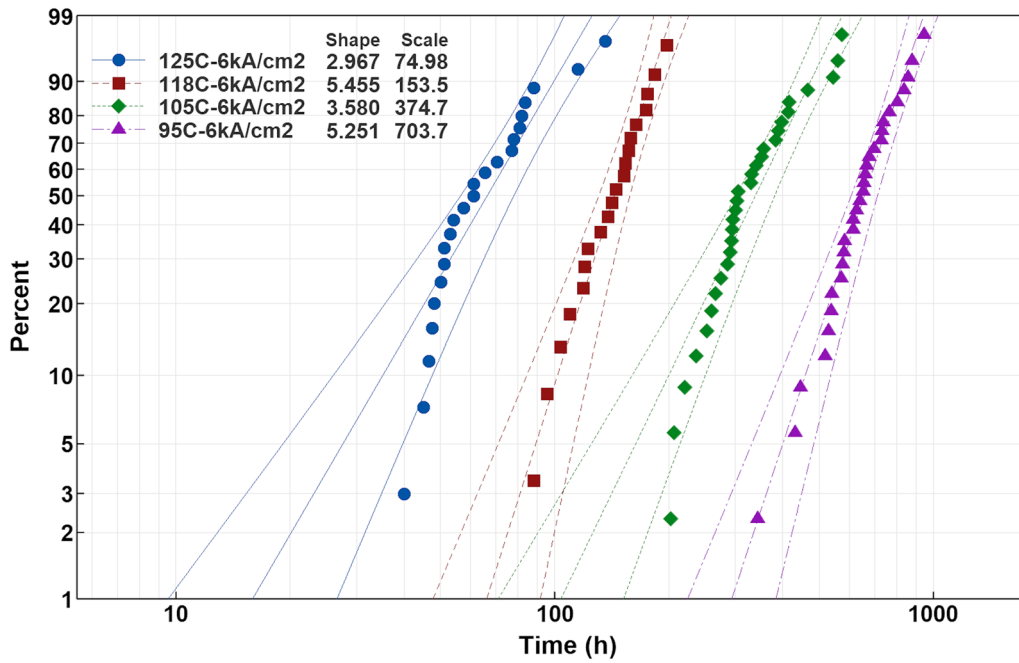


Fig. 7 Weibull distribution plots [95% confidence interval (CI)] for sample sets current-stressed with a current density of 6 kA/cm² and at one of four different temperatures from 95 to 125°C. The failure criterion was a 20% increase in the electrical resistance (four-terminal

measurement). The data from each sample are displayed in these plots of the percentage of samples failed versus current stressing time, along with the results of the Weibull fitting. The shape and scale for the Weibull fit for each dataset are displayed in the legend.

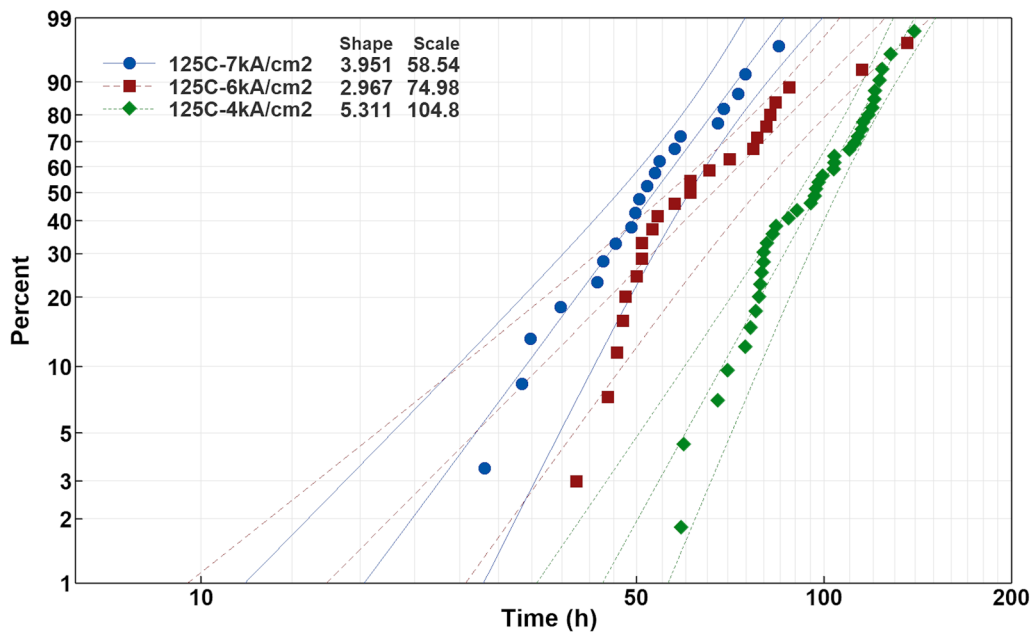


Fig. 8 Weibull distribution plots (95% CI) for sample sets current-stressed at a temperature of 125°C and at one of the current densities from 4 to 7 kA/cm². The failure criterion was a 20% increase in the electrical resistance (four-terminal measurement). The data from

each sample are displayed in these plots of the percentage of samples failed versus current stressing time, along with the results of the Weibull fitting. The shape and scale for the Weibull fit for each dataset are displayed in the legend.

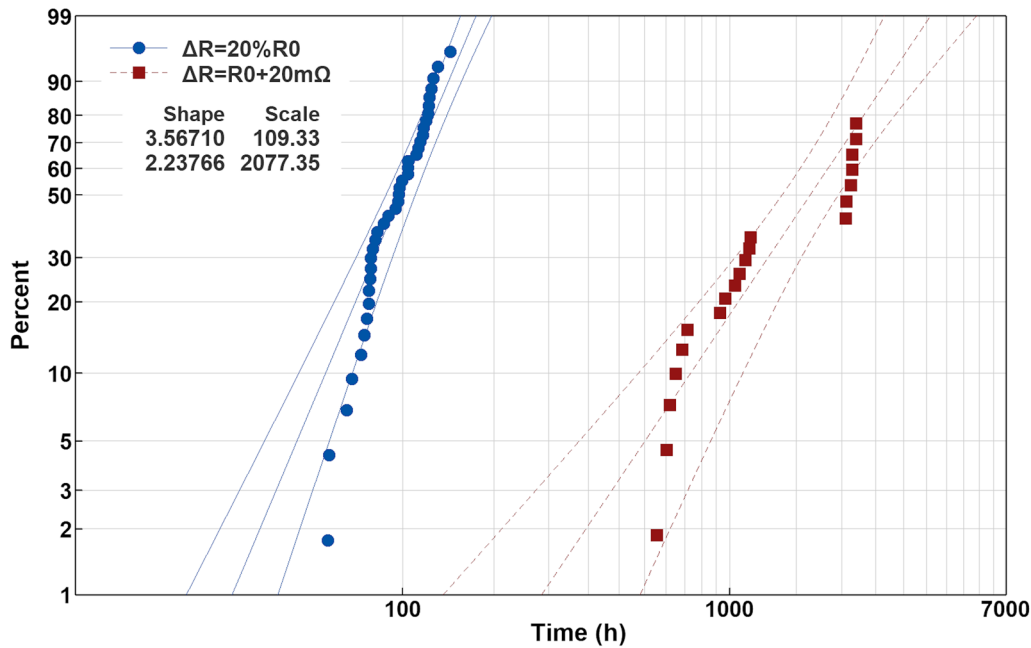


Fig. 9 Weibull distribution plots (95% CI) for a single set of samples which was current-stressed at a temperature of 125°C and at a current density of 4 kA/cm², the same dataset was analyzed with two different failure criteria: a 20% increase in electrical resistance (circles), and separately, a 20-mΩ increase in electrical resistance as measured

($R_0 + 20 \text{ m}\Omega$, where R_0 was the initial electrical resistance), that board was removed from the oven and the data for the rest of its joints were censored. An equal number of current down and current up catastrophic failures are reflected in the data (red squares) for catastrophic failure in Fig. 9. The MTF for current up samples was 1309 h, while the MTF for current down samples was 1485 h.

The source of the large difference in failure rates rested in the intrinsic difference in the atomic diffusion processes associated with each failure mechanism. As discussed above, failure by a 20% increase in electric resistance corresponded to electromigration of Bi, which occurred at a constant rate.²⁷ In contrast, the catastrophic failure mechanism rested upon the formation of Cu_6Sn_5 (failure occurred after complete consumption of Sn by Cu_6Sn_5 and formation of Bi interface), a diffusion-limited process with a rate that is not constant, a rate that monotonically decreases with time (proportional to the inverse of the thickness of the Cu_6Sn_5 , as has been observed many times previously). Thus, the MTF for catastrophic failure at a temperature of 125°C was more than 1000 h. As this failure rate is controlled by the rate of formation of Cu_6Sn_5 (a thermal process with an activation energy of approximately 0.8 eV/atom), the MTF would increase markedly with decreasing temperatures. Even at 90°C, at a current density of 2 kA/cm², extrapolation of the data from a temperature of 125°C (Fig. 9) indicates that, in a large sample set, a number of early failures would be expected in

with a four-terminal measurement (squares). The data from each sample are displayed in these plots of the percentage of samples failed versus current stressing time, along with the results of the Weibull fitting. The shape and scale for the Weibull fit for each dataset are displayed in the legend.

a year. It is clearly indicated that increased testing activity in a temperature range near 90°C, which corresponds to many expected field applications, is merited.

Conclusions

Two different failure criteria were used to examine the performance of Cu/Sn57BiSbNi/Ni solder joints during current stressing. Scanning electron microscopy was utilized to characterize changes observed in the solder joint microstructure. Thus, failure defined by a 20% increase in solder joint electrical resistance was correlated with Bi accumulation at the anode, and failure defined by a 20-mΩ increase in electrical resistance was correlated with catastrophic failure, as the solder joint cracked at a Bi interface. Each failure mechanism was identified with a different atomic diffusion process, and thus different kinetics. The statistics of these failure mechanisms were characterized with a Weibull analysis, and found to be distinct.

Acknowledgments The authors would like to express their gratitude to Michael Meilunas and Dr. Jim Wilcox of the Universal Instruments Advanced Process Laboratory for their assistance in sample preparation and useful technical discussion. Additional financial support from the IEEC and the Semiconductor Research Corporation (SRC) is also gratefully acknowledged.

Conflict of Interest The authors declare that there is no conflict of interest.

References

1. F. Wang, L. Liu, D. Li, and M. Wu, Electromigration behaviors in Sn-58Bi solder joints under different current densities and temperatures. *J. Mater. Sci. Mater. Electron.* 29, 21157 (2018).
2. R. Coyle, R. Aspandiar, M. Osterman, C. Johnson, R. Popowich, R. Parker, D. Hillman, N. Bell-labs, M. Hill, C. Park, and R. Collins: Alloy composition and thermal fatigue of high reliability Pb-free solder alloys, Proc. SMTA Int. Rosemont, IL, USA 17 (2017)
3. S.P. Lim, C. Arvin, D. Locker, R. Pokhrel, W.K. Loh, K. Sweatman, D. Daily, N. Kubota, and M. Tsuruya, Low temperature 1st level interconnect in packaging and its challenges. *Int Conf. Electron. Packag. ICEP 2021*, 49 (2021).
4. J. Glazer, Microstructure and mechanical properties of Pb-free solder alloys for low-cost electronic assembly: a review. *J. Electron. Mater.* 23, 693 (1994).
5. L.T. Chen, and C.M. Chen, Electromigration study in the eutectic SnBi solder joint on the Ni/Au metallization. *J. Mater. Res.* 21, 962 (2006).
6. S. Sahasrabudhe, S. Mokler, M. Renavikar, S. Sane, K. Byrd, E. Brigham, O. Jin, P. Goonetilleke, N. Badwe, and S. Parupalli: Low temperature solder – a breakthrough technology for surface mounted devices, In: *2018 IEEE 68th Electron. Components Technol. Conf.* 1455 (2018)
7. Y. Wang, X.C. Zhao, Y. Liu, J.W. Cheng, H. Li, and X.C. Xie, Effect of Bi addition on microstructures, properties and interfacial intermetallic compound growth of Low-Ag Sn-Cu lead-free solder. *Mater. Sci. Forum* 815, 109 (2015).
8. H. Takao, A. Yamada, and H. Hasegawa, Mechanical properties and solder joint reliability of Low-Melting Sn-Bi-Cu lead free solder alloy. *R&D Rev Toyota CRDL.* 39, 49 (2004).
9. R. Coyle, R. Aspandiar, M. Osterman, C. Johnson, R. Popowich, R. Parker, D. Hillman, N. Bell-labs, M. Hill, C. Park, and R. Collins: Thermal cycle reliability of a low silver ball grid array assembled with Tin Bismuth solder paste, *Proc. SMTA Int.* 72 (2017)
10. R. Coyle, R. Aspandiar, F. Hadian, S. Kempaiah, V. Vasudevan, A. Raj, P. Goonetilleke, D. Burkholder, M. Ribas, J. Radhakrishnan, C. Handwerker, H. Zhang, B. Arfaei, H. Fu, Q. Chen, D. Daily, M. Hill, I. Corporation, D. Technologies, R. Rock, P. Alto, M. Hill, and I. Corporation: Interim thermal cycling report on hybrid, homogeneous, and Resin reinforced low temperature solder joints *Proc. SMTA Int.* 401, (2021)
11. J. Zhao, L. Qi, X.M. Wang, and L. Wang, Influence of Bi on microstructures evolution and mechanical properties in Sn–Ag–Cu lead-free solder. *J. Alloys Comp.* 375, 196 (2004).
12. L. Zhang, L. Sun, and Y. Huan Guo, Microstructures and properties of Sn58Bi, Sn35Bi0.3Ag, Sn35Bi1.0Ag solder and solder joints. *J. Mater. Sci. Mater. Electron.* 26, 7629 (2015).
13. M. Ribas, A. Kumar, D. Kosuri, R. R. Rangaraju, P. Choudhury, S. Telu, and S. Sarkar: Low temperature soldering using Sn-Bi alloys. In: Proc. SMTA Int. (Rosemont, IL, 2017), pp. 201–206
14. M. Ribas, S. Chegudi, A. Kumar, R. Pandher, R. Raut, S. Mukherjee, S. Sarkar, and B. Singh: Development of low-temperature drop shock resistant solder alloys for handheld devices, In: Proc. 2013 IEEE 15th Electron. Packag. Technol. Conf. EPTC 2013 48 (2013)
15. X. Fu, Y. En, B. Zhou, S. Chen, Y. Huang, X. He, H. Chen, and R. Yao, Microstructure and grain orientation evolution in SnPb/SnAgCu interconnects under electrical current stressing at cryogenic temperature. *Materials* 12, 1593 (2019).
16. F. Wang, H. Chen, Y. Huang, and C. Yan, Interfacial behavior and joint strength of Sn–Bi solder with solid solution compositions. *J. Mater. Sci. Mater. Electron.* 29, 11409 (2018).
17. X. Zhao, M. Saka, M. Muraoka, M. Yamashita, and H. Hokazono, Electromigration behaviors and effects of addition elements on the formation of a Bi-rich Layer in Sn58Bi-based solders. *J. Electron. Mater.* 43, 4179 (2014).
18. F. Guo, G. Xu, J. Sun, Z. Xia, Y. Lei, Y. Shi, and X. Li, Resistance changes in eutectic Sn-Bi solder joints during electromigration. *J. Electron. Mater.* 38, 2756 (2009).
19. J. Sun, G. Xu, F. Guo, Z. Xia, Y. Lei, Y. Shi, X. Li, and X. Wang, Effects of electromigration on resistance changes in eutectic SnBi solder joints. *J. Mater. Sci.* 46, 3544 (2011).
20. X. Zhao, M. Muraoka, and M. Saka, Length-dependent electromigration behavior of Sn58Bi solder and critical length of electromigration. *J. Electron. Mater.* 46, 1287 (2017).
21. G. D. Pilin Liu, Fan-yi Ouyang, Shengquan Qu, Zezhong Fu: Solder joint electromigration mechanisms, In: *ASME 2009 InterPACK Conf. Proc. IPACK2009* (2019), pp. 1–7
22. JEDEC Solid State Technol. Assoc. (2011)
23. S.M. Lee, J.W. Yoon, and S.B. Jung, Electromigration effect on Sn-58 % Bi solder joints with various substrate metallizations under current stress. *J. Mater. Sci. Mater. Electron.* 27, 1105 (2016).
24. W.J. Choi, E.C.C. Yeh, and K.N. Tu, Mean-time-to-failure study of flip chip solder joints on Cu/Ni(V)/Al thin-film under-bump-metallization. *J. Appl. Phys.* 94, 5665 (2003).
25. J. Pan and J. Silk: A study of solder joint failure criteria, In: 44th Int. Symp. Microelectron. 2011, IMAPS 2011 2, 694 (2011)
26. F. Hadian, S. Panta, J. Flores, and E. J. Cotts: The effect of current stressing on the electrical resistance and microstructure of Sn-Bi based solder joints, *SMTA Int. Conf.* (2021), pp. 445–450
27. F. Hadian, J. Flores, and E. Cotts, The variation of the electrical resistance and microstructure of SnBi based solder joints with current stressing. *JOM* 74, 2139 (2022).
28. JEDEC, JESD33B, (2012)
29. A. Delhaise, *Solid-state diffusion of bismuth in Tin-Rich, Lead-Free Solder Alloys* (UK: University of Toronto, 2018).
30. S. Kumar, C.A. Handwerker, and M.A. Dayananda, Intrinsic and interdiffusion in Cu-Sn system. *J. Phase Equilib. Diffus.* 32, 309 (2011).

Publisher's Note Springer Nature remains neutral with regard to jurisdictional claims in published maps and institutional affiliations.

Springer Nature or its licensor (e.g. a society or other partner) holds exclusive rights to this article under a publishing agreement with the author(s) or other rightsholder(s); author self-archiving of the accepted manuscript version of this article is solely governed by the terms of such publishing agreement and applicable law.